Acta Crystallographica Section D
Biological Crystallography
ISSN 0907-4449

Crystallization and preliminary X-ray analysis of a membrane-bound nitrite reductase from *Desulfovibrio desulfuricans* ATCC 27774

João M. Dias,[a,b] Carlos A. Cunha,[a,b] Susana Teixeira,[a,b] Gabriela Almeida,[a] Cristina Costa,[a] Jorge Lampreia,[a] José J. G. Moura,[a] Isabel Moura[a] and Maria João Romão[a,b]*

[a]Departamento de Química, Centro de Química Fina e Biotecnologia, Faculdade de Ciências e Tecnologia, Universidade Nova de Lisboa, 2825-114 Monte de Caparica, Portugal, and [b]Instituto Tecnologia Química e Biológica, Apartado 127, 2780 Oeiras, Portugal

Correspondence e-mail: mromao@dq.fct.unl.pt

Received 28 September 1999
Accepted 8 December 1999

Nitrite reductase from the sulfate-reducing bacterium *Desulfovibrio desulfuricans* ATCC 27774 is a multihaem (type *c*) membrane-bound enzyme that catalyzes the dissimilatory conversion of nitrite to ammonia. Crystals of the oxidized form of this enzyme were obtained using PEG and $CaCl_2$ as precipitants in the presence of 3-(decylmethylammonium)propane-1-sulfonate and belong to the space group $P2_12_12_1$, with unit-cell parameters a = 78.94, b = 104.59, c = 143.18 Å. A complete data set to 2.30 Å resolution was collected using synchrotron radiation at the ESRF. However, the crystals may diffract to beyond 1.7 Å and high-resolution data will be collected in the near future.

1. Introduction

Nitrite reductases constitute a diverse group of enzymes with fundamental functions in the nitrogen biological cycle: denitrification, assimilation or dissimilation (Schumacher *et al.*, 1997; Brittain *et al.*, 1992; Zumft, 1997). The assimilatory enzymes are associated with the process of incorporating nitrogen for biosynthesis, while the dissimilatory enzymes use nitrogen as an alternative respiratory substrate. In the denitrification pathway, a copper-containing or a cytochrome cd_1-containing nitrite reductase initiate the sequential denitrification procedure, with the reduction of nitrite to NO in a two-electron step. In the assimilatory pathway, a sirohaem and iron–sulfur centres are present, and in the dissimilatory pathway, a multihaem cytochrome *c* type nitrite reductase catalyses the direct six-electron reduction of nitrite to ammonia.

Our studies concern the dissimilatory nitrite reductase (NIR) isolated from the sulfate-reducing bacterium *D. desulfuricans* ATCC 27774. Growing the bacteria with nitrate rather than sulfate induces NIR. It is a membrane-bound protein, first described as a 62 kDa monomer containing six haem *c* type prosthetic groups (Liu & Peck, 1981; Costa, Macedo *et al.*, 1990; Costa, Moura *et al.*, 1990; Costa *et al.*, 1996). Nevertheless, recent experiments showed the presence of an additional small 19 kDa subunit (Moura *et al.*, 1997; Almeida *et al.*, 1999) as determined by electrospray mass spectrometry and also by SDS–PAGE. A similar subunit was also identified in other cytochrome *c* nitrite reductases (*Escherichia coli, Wolinella succinogenes* and *Sulfurospirillum deleyanum*), which were also originally considered as hexahaemic (Darwin *et al.*, 1993; Berks *et al.*, 1995). However, the haem content was later established to be four in the case of *W. succinogenes* (Schumacher *et al.*, 1994) and five for the enzymes from *E. coli* and *S. deleyanum* (Eaves *et al.*, 1998; Einsle *et al.*, 1999).

The spectroscopic component of the nitrite reductase from *D. desulfuricans* was extensively characterized. Electron paramagnetic resonance and Mössbauer studies indicate a multihaem complex system (Costa, Moura *et al.*, 1990). Only one of the haems is in the high-spin electronic configuration (S = 5/2) and is assigned as the substrate-binding site. The other haems are in the low-spin state and two pairs (including the high-spin haem) are magnetically coupled, suggesting a close proximity between them.

2. Material and methods

2.1. Protein purification

The enzyme was extracted from *D. desulfuricans* as previously described (Liu *et al.*, 1994) by mild treatment of the membrane preparation with sodium choleate (4–6 mg l^{-1}) in 100 m*M* potassium phosphate buffer pH 7.6. The purification procedure was performed in two steps, a sequential ammonium sulfate fractionation (30–60%) and resuspension in potassium phosphate buffer, followed by HPLC/gel filtration on a Superdex 200 (Pharmacia) column equilibrated and eluted with 100 m*M* potassium phosphate pH 7.6 buffer. These purification steps do not require the presence of detergent, which suggests that the protein is not an integral membrane protein but a peripheral one. The nitrite reductase purity was checked by denaturant polyacrylamide electrophoresis and by UV–VIS

spectroscopy. SDS polyacrylamide (12.5%) mini-gel electrophoresis was carried out according to Laemmli (1970), using an EC unit. The samples were boiled for 2 min (without reducing agent, which could interfere with the subsequent haem staining) using the method of Goodhew *et al.* (1986).

2.2. Crystallization

The initial crystallization conditions were screened using an in-house modified version of the sparse-matrix method of Jancarik & Kim (1991), with and without the presence of detergents and amphiphilic molecules such as β-octyl-glucopyranoside, *n*-dodecyl-β-D-maltoside and 1,2,3-hexanetriol. The first experiments yielded multiple forms but very small crystals and these first assays showed that the presence of β-octyl-glucopyranoside was absolutely necessary.

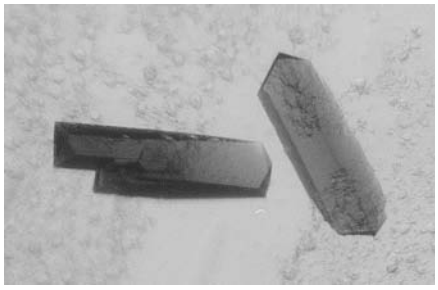

Figure 1
Crystals of nitrite reductase (NIR) from *D. desulfuricans* ATCC 27774 grown at 291 K. The crystals have approximate dimensions of 0.3 × 0.15 × 0.15 mm.

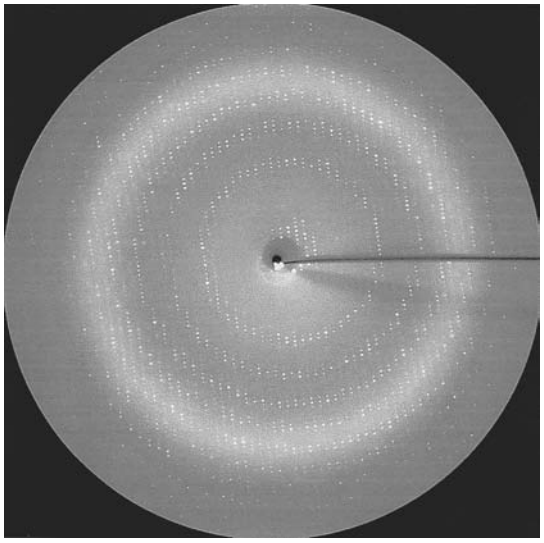

Figure 2
Typical diffraction pattern of a crystal of nitrite reductase from *D. desulfuricans* ATCC 27774. The edge of the image corresponds to 2.3 Å.

Crystals appeared using the following crystallization conditions in the presence of the detergent: 25% PEG 3350, 0.2 *M* $CaCl_2$, 0.1 *M* HEPES pH 7.5; 1.2 *M* sodium citrate, 0.1 *M* HEPES pH 7.5; 30% PEG 3350, 0.2 *M* Li_2SO_4, 0.1 *M* citrate pH 5.5; 30% MPD, 0.2 *M* ammonium phosphate, 0.1 *M* Tris pH 7.5; 30% PEG 3350, 0.2 *M* sodium acetate, 0.1 *M* Tris pH 7.5; 20% PEG 3350, 10% 2-propanol, 0.1 *M* HEPES pH 7.5. However, the reproducibility of the best initial conditions was difficult, temperature sensitive and very much dependent on the protein batch.

Further studies were carried out in order to improve and reproduce some of the crystallization conditions using sulfobetaines [zwitterionic surfactants (Gonenne & Ernst, 1978) such as dimethyl ethylammonium propane sulfonate (Vuillard *et al.*, 1994)] in combination with β-octyl-glucopyranoside. Other screenings were also performed in parallel with the commercial Hampton Research (California, USA) Crystal Screen and Crystal Screen 2 in conjunction with the addition of several detergents from the Hampton Research detergent-screening kit (California, USA). The best results were achieved using Zwittergent 3-10 [3-(decyl-methylammonium)propane-1-sulfonate] or MEGA-8 (octanoyl-*N*-methylglucamide). The optimized conditions were then restricted to 25% PEG 3350, 0.2 *M* $CaCl_2$, 0.1 *M* HEPES pH 7.5, detergent Zwittergent 3-10 or 30% PEG 3350, 0.2 *M* ammonium acetate, 0.1 *M* citrate pH 5.5, MEGA-8. Crystallization assays were carried out under these conditions at several constant temperatures (277, 285, 291, 294 and 303 K) using the hanging-drop and sitting-drop vapour-diffusion methods. Different buffers and additives did not improve the crystallization conditions and seeding techniques were not successful, as both microseeding and macroseeding suffered from protein aggregation. The crystal quality was finally improved by changing the PEG concentration as well as the temperature and detergent.

The best large crystals were obtained using 4 µl of a 10 mg ml^{-1} protein solution, 1 µl of a 400 m*M* solution of Zwittergent 3-10 and 5 µl of a reservoir solution containing 15% PEG 3350, 0.2 *M* $CaCl_2$, 0.1 *M* HEPES buffer pH 7.5. At room temperature (291 K), the crystals grow in one month to dimensions of 0.3 × 0.15 × 0.15 mm (Fig. 1).

2.3. Data collection and reduction

Cryoprotection of the NIR crystals was crucial for complete data collection and effectively eliminated radiation damage to the crystals. A number of different cryoprotectant solutions at different concentrations had to be tried, including glycerol, PEG 400 and ethylene glycol. Satisfactory freezing of the NIR crystals was achieved with a cryoprotectant solution containing 25% ethylene glycol, 20% PEG 3350, 0.1 *M* HEPES buffer pH 7.5, 0.2 *M* $CaCl_2$ and Zwittergent 3-10. The most efficient protocol was to first add the harvesting buffer (of similar composition to the cryoprotectant solution but without ethylene glycol) to the crystal drop and then to transfer the crystal to a new drop of harvesting buffer. The cryoprotectant solution was then slowly added to this drop and, after equilibration, the crystal was transferred to a new drop of cryoprotectant and then rapidly mounted in a cryoloop followed by flash-freezing in a stream of cooled nitrogen gas maintained at 100 K throughout data collection.

A complete data set was collected on an X-ray imaging-plate system using synchrotron radiation at the European Synchrotron Radiation Facility (ESRF) beamline ID14, with resolution to 2.3 Å. A typical rotation photograph taken from an NIR crystal is shown in Fig. 2.

3. Results and discussion

Careful SDS–PAGE comparison pattern analysis of native protein and dissolved NIR crystals indicates that the small subunit is not present in the crystalline material. The crystals only contain the large subunit, suggesting that dissociation occurred upon crystallization. The crystals are orthorhombic and, based on the systematic absences from collected data, belong to space group $P2_12_12_1$, with unit-cell parameters a = 78.94, b = 104.59, c = 143.18 Å. One particular crystal diffracted to beyond 1.7 Å, but unfortunately it was multiple. Using a single crystal, it was possible to collect a data set complete to 2.3 Å resolution. The data were processed with the program packages *DENZO* and *SCALEPACK* (Otwinowski & Minor, 1997), with 52 290 unique reflections from 686 901 independent measurements with an overall completeness of 97.4% in the resolution range 30.0–2.3 Å and an overall $R_{\rm merge}$ of 9.2%, with $R_{\rm merge}$ of 43.5% for the last shell (2.40–2.30 Å). A summary of the data-

Table 1
Crystal data and data-collection statistics.

Crystal data	
Space group	$P2_12_12_1$
Unit-cell parameters (Å)	a = 78.94, b = 104.59, c = 143.18
Data collection	
Resolution (Å)	30.0–2.30
Last resolution shell (Å)	2.40–2.30
Number of observations	686901
Number of unique reflections	52290
R_{merge} (%)	9.2
Last resolution shell (%)	43.5
Completeness (%)	97.4
Last resolution shell (%)	89.8
$I/\sigma(I)$	15.5
Last resolution shell	2.8

collection and final processing statistics is shown in Table 1.

According to the cell size and symmetry, calculation of the solvent content (Matthews, 1968) suggests that there could be two molecules of the large subunit of 62 kDa of NIR per asymmetric unit, with a corresponding Matthews ratio, V_M, of 2.38 Å^3 Da^{-1}. This is within the average V_M values found for protein crystals and indicates a solvent content of approximately 48.0%.

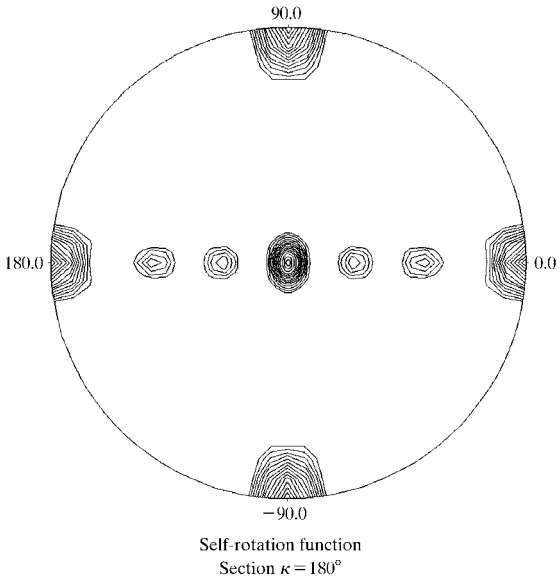

Figure 3
Stereographic plot of the κ = 180° section of the self-rotation function (calculated with *POLARRFN* from the *CCP*4 package) for the nitrite reductase native data (20–4 Å).

In order to clarify the presence of a dimer and to search for the non-crystallographic axis, the self-rotation function was calculated using *POLARRFN* from the *CCP*4 package (Collaborative Computational Project, Number 4, 1994). The results are depicted as a (φ, ψ) stereogram (Fig. 3) for one section of κ = 180°. This section shows evidence for the non-crystallographic twofold axis generating the dimer structure.

We have now collected MAD data at the ESRF beamline BM14 on the iron absorption edge because of the presence of haem iron; these data are being analysed in order to obtain independent experimental phases. These data will allow us to solve the NIR structure and answer some of the questions raised by the biochemical and spectroscopic studies, thus contributing to clarification of the role of multihaem membrane-bound nitrite reductases in sulfate-reducing bacteria.

This work was supported in part by PRAXIS XXI projects 2/2.1/BIO/05/94 and 2/2.1/QUI/3/94 and the EC-TMR ERB-FMRX-CT980204 and PhD grants PRAXIS XXI/BD/13530/97 (JMD) and PRAXIS XXI/BD/15752/98 (CAC). We would like to thank the EMBL Grenoble Outstation and the support for measurements at the ESRF under the European Union TMR/LSF Programme.

References

Almeida, G., Lampreia, J., Moura, J. J. G. & Moura, I. (1999). *J. Inorg. Biochem.* **74**, 63.
Berks, B. C., Ferguson, S. J., Moir, J. W. B. & Richardson, D. J. (1995). *Biochim. Biophys. Acta*, **1232**, 97–173.
Brittain, T., Blackmore, R., Greenwood, C. & Thomson, A. J. (1992). *Eur. J. Biochem.* **209**, 792–802.
Collaborative Computational Project, Number 4, (1994). *Acta Cryst.* D**50**, 760–763.
Costa, C., Macedo, A., Moura, I., Moura, J. J. G., LeGall, J., Berlier, Y., Liu, M. Y. & Payne, W. J. (1990). *FEBS Lett.* **276**, 67–70.
Costa, C., Moura, J. J. G., Moura, I., Liu, M. Y., Peck, H. D., LeGall, J., Wang, Y. & Huynh, B. H. (1990). *J. Biol. Chem.* **265**, 14382–14387.
Costa, C., Moura, J. J. G., Moura, I., Wang, Y. & Huynh, B. H. (1996). *J. Biol. Chem.* **271**, 23191–23196.
Darwin, A., Hussein, H., Griffiths, L., Grove, J., Sambongi, Y., Busby, S. & Cole, J. (1993). *Mol. Microbiol.* **9**, 6, 1255–1265.
Eaves, D. J., Grove, J., Staudenmann, W., James, P., Poole, R. K., White, S. A., Griffiths, I. & Cole, J. A. (1998). *Mol. Microbiol.* **28**, 205–216.
Einsle, O., Messerschmidt, A., Stach, P., Huber, R. & Kroneck, P. (1999). *J. Inorg. Biochem.* **74**, 121.
Gonenne, A. & Ernst, R. (1978). *Anal. Biochem.* **87**, 23–38.
Goodhew, C. F., Brown, K. R. & Pettigrew, G. W. (1986). *Biochim. Biophys. Acta*, **852**, 288–294.
Jancarik, J. & Kim, S.-H. (1991). *J. Appl. Cryst.* **24**, 409–411.
Laemmli, U. K. (1970). *Nature (London)*, **227**, 680–685.
Liu, M. C., Costa, C. & Moura, I. (1994). *Methods Enzymol.* **243**, 303–319.
Liu, M. C. & Peck, H. D. Jr (1981). *J. Biol. Chem.* **256**, 13159–13164.
Matthews, B. W. (1968). *J. Mol. Biol.* **33**, 491–497.
Moura, I., Bursakov, S., Costa, C. & Moura, J. J. G. (1997). *Anaerobe*, **3**, 279–290.
Otwinowski, Z. & Minor, W. (1997). *Methods Enzymol.* **276**, 307–326.
Schumacher, W., Hole, U. & Kroneck, P. M. H. (1994). *Biochem. Biophys. Res. Commun.* **205**(1), 911–916.
Schumacher, W., Neese, F., Hole, U. & Kroneck, M. H. (1997). *Transition Metals in Microbial Metabolism*, edited by G. Winkelmann & C. J. Carrano, pp. 329–356. London: Harwood Academic Publishers.
Vuillard, L., Rabilloud, T., Leberman, R., Berthet-Colominas, C. & Cusack, S. (1994). *FEBS Lett.* **353**, 294–296.
Zumft, W. G. (1997). *Microbiol. Mol. Biol. Rev.* **61**, 533–616.